ACS OMEGA

Article

Cite This: ACS Omega 2019, 4, 14962−14969

http://pubs.acs.org/journal/acsodf

Capric Acid Hybridizing Fly Ash and Carbon Nanotubes as a Novel Shape-Stabilized Phase Change Material for Thermal Energy Storage

Peng Liu,[†,‡] Xiaobin Gu,[*,§] Zhikai Zhang,[*,‡] Jun Rao,[‡] Jianping Shi,[∥] Bin Wang,[†] and Liang Bian[†,‡]

[†]Key Laboratory of Solid Waste Treatment and Resource Recycle, Ministry of Education, South West University of Science and Technology, Mianyang 621010, Sichuan, China

[‡]School of Gemology and Materials Technology, Hebei GEO University, Shijiazhuang 050031, Hebei, China

[§]Materials and Interfaces Center, Shenzhen Institutes of Advanced Technology, Chinese Academy of Sciences, Shenzhen 518005, Guangdong, China

[∥]School of Electronic & Communication Engineering, Guiyang University, Guiyang 550005, China

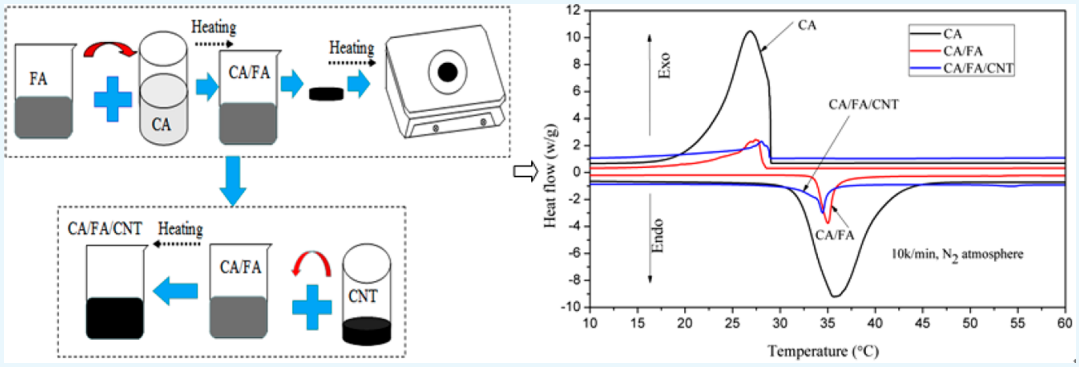

ABSTRACT: Capric acid (CA) is one of the most promising phase change materials to be used in reducing the energy consumption of buildings due to its suitable phase change temperature and high latent heat. In this paper, a novel shape-stabilized phase change material (SSPCM) is fabricated by "hazardous waste" fly ash (FA) via simple impregnation method along with CA and carbon nanotubes (CNTs). In this composite, raw FA without any modification serves as the carrier matrix to improve structural strength and overcome the drawback of the leakage of liquid CA. Simultaneously, CNTs act as an additive to increase the thermal conductivity of composites. The results of leakage tests indicate that CA was successfully confined as 20 wt % in the composite. Then, various characterization techniques were adopted to investigate the structure and properties of the prepared SSPCM of CA/FA/CNT. Scanning electron microscopy and Fourier transform infrared spectroscopy results showed that CA was well adsorbed into the microstructure of FA, and there was no chemical interaction between the components of the composites. Thermogravimetric analysis results demonstrated that the SSPCM presented good thermal stability. Differential scanning calorimetry results indicated that the melting temperature and freezing temperature of CA/FA/CNT were 31.08 and 27.88 °C, respectively, and the latent heats of CA/FA/CNT during the melting and freezing processes were 20.54 and 20.19 J g^{-1}, respectively. Moreover, compared to the CA and CA/FA, the heat transfer efficiency of CA/FA/CNT was significantly improved by doping 1, 3, 5, and 7 wt % of CNT. All of the results suggest that CA/FA/CNT possessed comfortable melting and freezing temperatures, excellent thermal stability, high latent heat value, and favorable thermal conductivity, and therefore, it is a suitable thermal storage material for building applications. Simultaneously, CA/FA/CNT can improve the comprehensive utilization level of FA.

1. INTRODUCTION

In recent years, with rapidly increasing and huge energy demand such as energy consumption of buildings,[1,2] improper utilization of fossil energy such as oil and coal inevitably results in serious environmental pollution. Taking the unclean use of coal as an example, combustion as the main utilization of coal brings about a large amount of solid waste—fly ash (FA). Particularly, in thermal power plants, during the coal-fired power generation process, a large amount of fly ash is generated. Therefore, conserving energy and developing new energy are imperative to protect the environment. However, the problems of low efficiency and poor supply stability seriously restrict the large-scale application of renewable energy. Fortunately, thermal energy storage is an effective solution for the utilization efficiency and stability of renewable energy sources. Therefore, thermal storage technologies have been developed to overcome this issue. Compared to other types, latent heat storage, which can store or release energy

Received: June 13, 2019
Accepted: August 12, 2019
Published: September 5, 2019

DOI: 10.1021/acsomega.9b01746
ACS Omega 2019, 4, 14962−14969

Table 1. Comparison of Mineral Components between FA and Some Typical Natural Minerals[32,33]

item	SiO_2	Al_2O_3	Fe_2O_3	CaO	MgO	$K_2O + Na_2O$	others
FA	43−56	20−35	4−10	0.5−1.5	0.6−2	1−2.5	3−20
diatomite	97.91	1.04	0.65		0.05	0.12	0.23
perlite	74.6	13.1	0.83	0.83	0.19	7.87	2.58

during the phase change process, is considered to be a promising type of heat storage.[2] In the investigated thermal storage technologies during the latent heat storage process, phase change material (PCM) is the most popularly working medium owing to its high energy storage density, phase transition at constant temperature, reversible phase change process, and thermal stability. Among the investigated PCMs, the fatty acids, as one kind of typical PCMs, are commonly preferred for latent heat energy storage due to their excellent properties such as suitable phase change temperature, high heat latent value, almost no supercooling, nontoxic, and so on.[3,4]

However, the drawbacks of the leakage problem during melted state and low thermal conductivity of fatty acid significantly limit their practical applications.[5] Therefore, lots of work have been done to overcome these drawbacks. Usually, fatty acids are encapsulated into macro- or microdimension structure, namely, microencapsulation technology.[5−7] However, the microencapsulation technology is relatively more complex with higher cost and lower thermal storage capacity. Compared to the microencapsulation technology, another option is to form stable encapsulation of PCM by using porous minerals with developed pore structure, lightweight, and low cost, such as kaolinite,[8,9] graphite,[10−12] perlite,[13] meteorite,[14] and diatomite.[15−18] Construction of porous material absorption systems has been demonstrated by many researchers, and the previous work has proved that it can effectively solve the liquid leakage problem and protect PCM from external problems. On the other hand, to increase the thermal conductivity of fatty acids, many high thermal conductivity materials have been applied, such as carbon nanotubes (CNTs),[3,19] which are homogeneously mixed with fatty acids.[20] The superior properties and feasibility of CNT enhancer have been confirmed by many studies.[21−25]

Fly ash (FA) is the byproduct of coal-fired power generation in a thermal power plant. Particularly, in China, where coal is used as the main energy source, thermal power accounts for more than 50% of the whole electricity consumption. In 2015, the annual discharge of FA is about 6.2×10^8 t in China. The treatment and comprehensive utilization of FA have been one of the hot social topics. Fortunately, FA possesses many similar properties with some porous mineral that enables it to act as a carrier matrix to prevent the leakage of melted fatty acid. Moreover, initial exploration studies have confirmed the feasibility of this experiment.[26−30] However, a lot of work still needs to be done to evaluate the properties of FA-based PCM.

In this study, we aim to develop a novel shape-stabilized phase change material (SSPCM) by a facile synthetic method of direct impregnation. Capric acid (CA) is considered to be one of the most promising fatty acids for the most suitable phase change temperature approximate to human comfortable temperature and high latent heat capacity. CNT, as a kind of lightweight carbon material with high thermal conductivity, has been widely used as the thermal conductivity enhancer of PCM. Therefore, in this composite, the CA with a comfortable temperature range and high latent heat acts as PCM. And raw FA and CNT serve as the carrier matrix and thermal conductivity enhancer, respectively. The various characteristic techniques were used to investigate the thermal properties of these composites.

2. RESULTS AND DISCUSSION

2.1. Theoretical Feasibility Analyses of FA Used for Support Material. The natural minerals can act as carrier matrix due to the main characteristic of the porous structure. In detail, the components in the natural mineral have different lattice structures and crystal structures, which provide more pore structure and larger specific surface area. Thus, the fatty acid and natural minerals could be tightly combined by forces such as capillary force, tension force, and drag force.[31] Owing to the similar mineral components and pore structure between FA and some typical natural minerals, FA can also be used as a carrier matrix in theory. A comparison of mineral components between FA and some typical porous minerals is given in Table 1. As can be seen from Table 1, mineral components in FA are almost the same as those in some typical natural minerals. The mineral components such as SiO_2, Al_2O_3, and MgO may be used as porous material, whereas the components such as Na_2O and K_2O have a fluxing effect, which makes FA possible to be used as supporting material of PCM. Therefore, acting as carrier matrix of PCM is a new approach for the comprehensive utilization of fly ash.

2.2. Morphology of the CA/FA/CNT SSPCM. Scanning electron microscopy (SEM) images of CA, FA, CNT, CA/FA PCM, and CA/FA/CNT are shown in Figure 1. As can be seen from Figure 1a−c, CA exhibits a viscous-liquid-like glue due to the lower phase-transition temperature. And FA has microsphere structures like hairy spheres with different diameters. The CNT with abundant pore structures was similar to cotton wool due to agglomeration between particles. As seen from Figure 1d, after FA is impregnated with CA, the microsphere structure surface of FA was covered by the impregnated CA to a certain extent. CA/FA SSPCM reveals significant difference from FA. This displays that specific amount of CA can be adsorbed into microstructure or covered on the surface of the sphere of FA owing to surface forces. In other words, it may be the reason that FA could prevent the leakage of melted CA. It can be clearly observed from Figure 1e,f that the CNT is mixed with CA and covered on the surface of FA or filled between spherical particles of fly ash, which indicates that the CNT can successfully construct path channels for heat transfer between CA and CA in comparison to CA/FA.

2.3. Chemical Compatibility of CA/FA/CNT SSPCM. Figure 2 illustrates the Fourier transform infrared (FTIR) spectra of CA, FA, CNT, CA/FA SSPCM, and CA/FA/CNT SSPCM selected as samples on behalf of other composites. As seen in Figure 2, in the spectrum of CA, the peaks at 939, 1410, and 1710 cm^{-1} represent stretching vibrations of −OH, C═O, and COO− groups, respectively. Besides these peaks, 2850 and 2930 cm^{-1} can be ascribed to the symmetric stretching vibrations of $-CH_3$ and $-CH_2$ groups, respec-

DOI: 10.1021/acsomega.9b01746
ACS Omega 2019, 4, 14962−14969

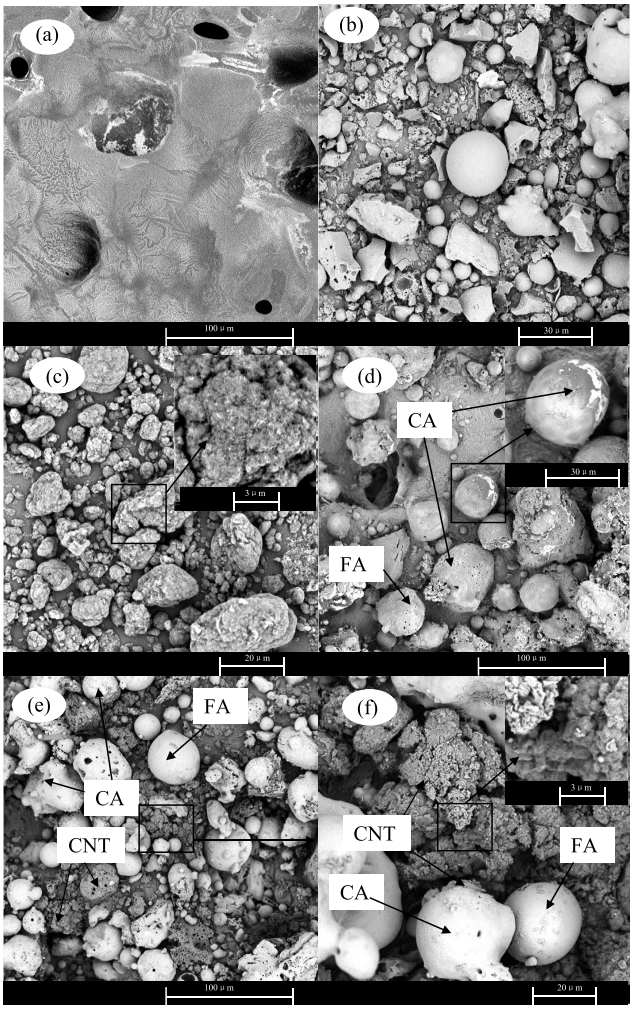

Figure 1. SEM images of CA (a), FA (b), CNT(c), CA/FA (d), and CA/FA/CNT (e, f).

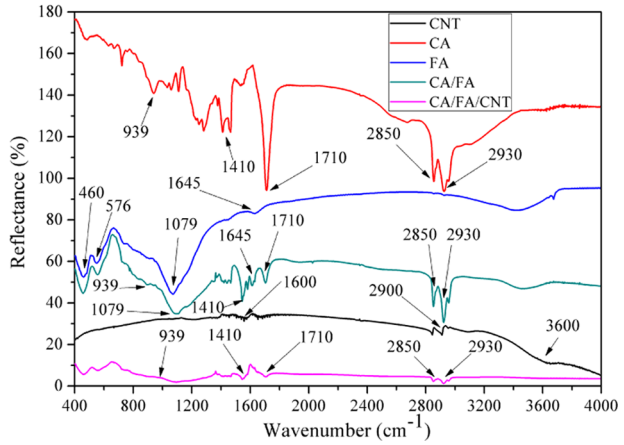

Figure 2. FTIR spectra of CA, FA, CA/FA, and CA/FA/CNT.

tively.[34,35] The FTIR spectrum of FA, which shows peaks at 460, 576, 1079, and 1645 cm^{-1}, signifies the stretching vibrations of O−Si−O, Si−O−Si, Si−O−Al, and O−H, respectively.[28] In the spectrum of CNT, the main absorption bands at 1600, 2900, and 3600 cm^{-1} are assigned to the stretching vibration bands of −C═C−, −C−H, and −O−H (due to humidity content), respectively.[3,19] On the other hand, from the FTIR spectrum of CA/FA SSPCM and CA/FA/CNT, it could be clearly observed for all of the characteristic peaks which appeared in the curves of CA, FA, and CNT, there are no obviously new characteristic peaks, which suggests that the interaction between CA, FA, and CNT was only a physical process and the components in the SSPCM have good chemical compatibility.

2.4. Thermal Properties of CA/FA/CNT SSPCM. The thermal properties of CA, CA/FA SSPCM, and CA/FA/CNT SSPCM were determined by differential scanning calorimetry (DSC), and the DSC curves are shown in Figure 3 and Table

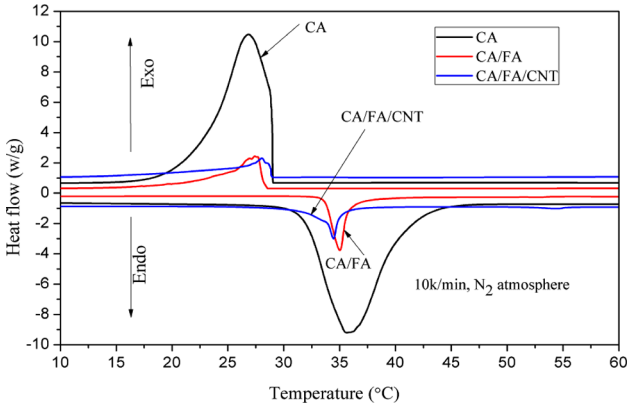

Figure 3. DSC curves of CA, CA/FA, and CA/FA/CNT.

2. As easily observed from Figure 3 and Table 2, the melting temperature and solidifying temperature of CA are 35.89 and 26.84 °C, with latent heat values of 169.5 and 167.6 J g^{-1}, respectively. The melting and freezing temperatures were determined as 31.53 and 28.17 °C, respectively, for CA/FA SSPCM whereas they were measured as 31.08 and 27.88 °C for CA/FA/CNT SSPCM. Compared to the pure CA, there are minor deviations in melting temperature between 31.08 and 35.89 °C and in solidifying temperature between 26.84 and 28.17 °C due to the weak physical interaction among the components of composites. Fortunately, the melting/solidifying temperatures are more suitable for human body comfort and closer to the comfortable room temperature range of 16−26 °C. The advantage is that CA can be used as PCM for thermal storage application in buildings.

On the other hand, as can be seen from Figure 3 and Table 2, the latent heat capacities of melting and solidifying were measured as 24.40 and 24.66 J g^{-1} for CA/FA SSPCM, 20.54 and 20.19 J g^{-1} for CA/FA/CNT SSPCM, respectively. And the latent heat values of CA/FA/CNT SSPCM were slightly lower than those of CA/FA SSPCM. This indicates that the CNT enhancer has no remarkable dropping effect on latent heat values of CA/FA/CNT.

Compared to latent heats found in some studies, the latent heats of the prepared SSPCM in this study were higher than those of some other SSPCM reported in the literature.[36−40] The comparison results are also presented in Table 2. Therefore, it can be concluded that the suitable phase change temperature and high latent heat value of CA/FA/CNT make it more suitable for TES as ingredients material in buildings.

2.5. Thermal Stability of CA/FA/CNT SSPCM. Thermogravimetric analysis (TGA) was used to estimate the thermal stability of the fabricated SSPCM, and the obtained results are illustrated in Figure 4. As seen from the curves in

DOI: 10.1021/acsomega.9b01746
ACS Omega 2019, 4, 14962−14969

Table 2. Thermal Properties and Results Comparisons with Some Studies

sample	melting temperature (°C)	latent heat of melting (J g^{-1})	solidifying temperature (°C)	latent heat of solidifying (J g^{-1})	thermal conductivity (W m^{-1} K^{-1})
capric/myristic acid (20.0 wt %) + vermiculite	19.8	27.46	17.1	31.42	36
capric−myristic acid (20.0 wt %)/vermiculite +2 wt % expanded graphite	19.7	17.1	26.9		36
capric−lauric acid (25−30 wt %) + fire retardant /gypsum	17.0	21.0	28.0		37
paraffin (18 wt %)/kaolin	23.9	26.3	27.9		38
xylitol pentalaurate (19 wt %)/cement	44.07	41.08	31.09	27.36	39
xylitol pentalaurate (20 wt %)/gypsum	40.44	39.53	31.77	29.47	39
PA (25 wt %)/active aluminum oxide	74.13	59.57	28.56	17.53	40
CA	35.89	169.5	26.84	167.6	this study
CA (20 wt %)/FA	31.53	24.40	28.17	24.66	this study
CA (20 wt %)/FA/CNT	31.08	20.54	27.88	20.19	this study

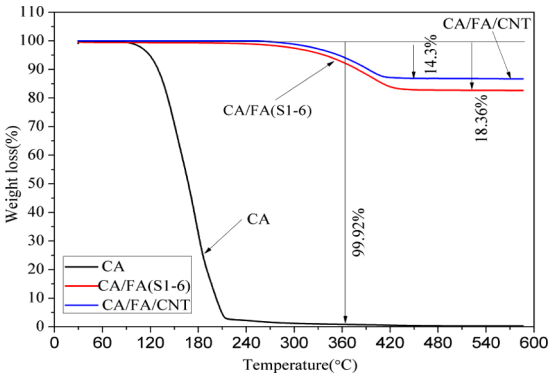

Figure 4. TGA curves of CA, CA/FA, and CA/FA/CNT.

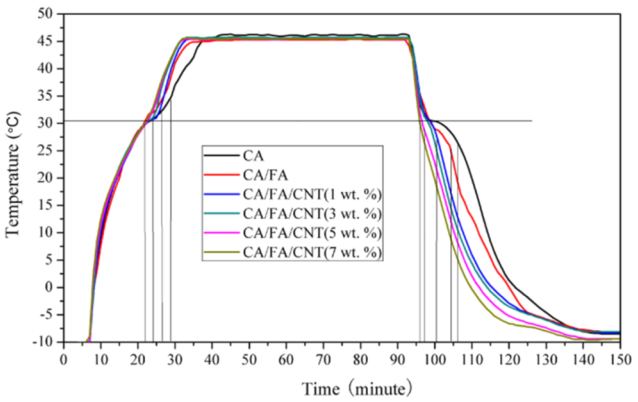

Figure 5. Storage and release curves of CA, CA/FA, and CA/FA/CNT.

Figure 4, there is a single degradation process 80−320 °C for CA due to the decomposition of fatty acid. The mass loss percentage of CA was 99.92%, whereas the thermal degradation temperature limits (°C) of CA/FA SSPCM and CA/FA/CNT are around 230 and 240 °C respectively, which are much higher than their working temperatures (16−26 °C). Moreover, the mass loss ratios of CA/FA SSPCM and CA/FA/CNT are about 18.36 and 14.30% at temperatures 420 and 440 °C, respectively. In addition, the weight loss for SSPCM is almost equal to the incorporation amounts of CA in each SSPCM. This finding reveals that the FA is feasible to serve as the carrier matrix of PCM. Good thermal stabilities of CA/FA SSPCM and CA/FA/CNT make them more suitable for application in buildings.

2.6. Thermal Storage/Release Performance of the CA/FA/CNT SSPCM. The thermal storage/release performance also revealed the heat transfer efficiency. The melting and cooling curves of CA, CA/FA SSPCM, and CA/FA/CNT are shown in Figure 5 by thermal storage/release tests. The test method of the melting and cooling curve in this study is the same as the conditions in our previous report.[18] To evaluate whether the storage efficiency of CNT composite is better than the other composites without CNT or not, the time length of the melting/freezing process (time from initial time/phase change point to the phase change point/termination time) and the time length of phase change constant temperature during the melting/freezing process can usually be considered as the evaluation parameter. As it can be seen from Figure 5, during the melting process, it takes about 15, 13, 13, 12, 12, and 11 min for CA, CA/FA, CA/FA/CNT (1 wt %), CA/FA/CNT (3 wt %), CA/FA/CNT (5 wt %), and CA/FA/CNT (7 wt %) to increase temperature from 16 to 32 °C, respectively. Compared to CA, CA/FA SSPCM, the melting time of CA/FA/CNT was reduced by 26.67 and 15.38%, respectively. Similarly, during the solidifying process, it takes about 14, 9, 7, 6, 5, and 4 min for CA, CA/FA, CA/FA/CNT (1 wt %), CA/FA/CNT (3 wt %), CA/FA/CNT (5 wt %), and CA/FA/CNT (7 wt %) to decrease temperature from 32 to 16 °C, respectively. In comparison to CA, CA/FA PSPCM, the solidifying time of CA/FA/CNT was reduced by 71.43 and 55.56%, respectively. In addition, during the melting process, the maintaining times of equilibrium temperature platform of CA, CA/FA, CA/FA/CNT (1 wt %), CA/FA/CNT (3 wt %), CA/FA/CNT (5 wt %), and CA/FA/CNT (7 wt %) are about 12, 7, 5, 3.5, 2.5, and 2 min, respectively. And in the solidifying process, it takes about 11, 6, 4, 2.5, 2, and 2 min for CA, CA/FA, CA/FA/CNT (1 wt %), CA/FA/CNT (3 wt %), CA/FA/CNT (5 wt %), and CA/FA/CNT (7 wt %) to maintain equilibrium temperature platform, respectively. Correspondingly, the maintaining time of equilibrium temperature platform of CA/FA/CNT (7 wt %) is less than that of CA and CA/FA by 83.33 and 71.43% for thermal storage and 81.82 and 66.67% for thermal release, respectively. All of the results also confirm that CNT enhancer in PSPCM can obviously improve the heat transfer efficiency.

3. CONCLUSIONS

To overcome the drawbacks of leakage and low thermal conductivity of CA, a novel SSPCM of CA/FA/CNT was fabricated via the facile direct impregnation method. The microstructure, chemical compatibility, thermal properties, thermal stability, thermal conductivity, and thermal storage/

DOI: 10.1021/acsomega.9b01746
ACS Omega 2019, 4, 14962−14969

release performance of prepared SSPCM were investigated. The CA can be successfully adsorbed by FA in a maximum fraction of 20 wt % without leakage of CA. The SEM and FTIR analyses confirmed that there was no chemical reaction among the components in SSPCM. The DSC results revealed that the CA/FA/CNT had a phase change temperature of 31.08 °C for the melting process and 27.88 °C for the solidifying process as they indicated latent heat changed 20.54 J g^{-1} for melting process and 20.19 J g^{-1} for the solidifying process. The TGA analysis showed that CA/FA/CNT had good thermal stability above its working temperature. Moreover, the charging/discharging time of CA/FA/CNT was shorted owing to the improved thermal conductivity by CNT enhancer. In short, CA/FA/CNT has great potential in buildings for thermal storage as ingredient material. At the same time, it could provide a new approach for the comprehensive utilization of FA.

4. EXPERIMENTAL SECTION

4.1. Materials. CA was provided from Sinopharm Chemical Reagent Co., Ltd (Shanghai, China). The FA was supplied by the Hebei Thermal Power Plant (Shijiazhuang, China). The granulated FA sample was sieved using 0.250 mm mesh and then dried at 110 °C for 2 h to remove the humidity. The CNT was obtained from Suzhou Tanfeng Graphene Technology Co., Ltd (Suzhou, China).

4.2. Preparation of SSPCM. The SSPCM of CA/FA/CNT sample used in this study was prepared by the direct impregnation method. The preparation process of the composite can be concluded in two steps, as shown in Figure 6. In the first step, the weighed CA and FA were put into a 25

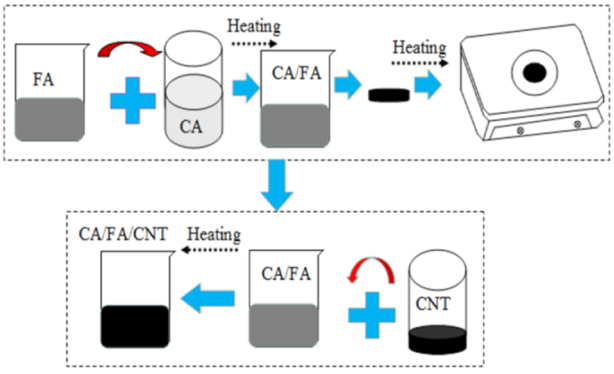

Figure 6. Preparation process of PA/FA/CNT.

mL beaker and evenly mixed. Then, the mixture was heated at 60 °C for 10 min and slowly hand-stirred continuously. After that, the sample was cooled to 20 °C for 2 h to obtain the fabricated composite. And then the leakage tests of CA/FA were carried out according to the effective method reported in the literature.[41] For this purpose, samples including the different amounts of CA were heated on filter papers by checking the leakage case. The sample tablets of CA/FA composites used for the leakage test are shown in Figure 7, and the results are presented in Figures 8 and 9. In the next step, the SSPCM CA/FA without liquid leakage at a specific weight was added in powder form into 25 mL beakers and mixed with the CNT with different mass fractions, respectively. Then, the mixture was heated at 60 °C for 10 min and slowly stirred.

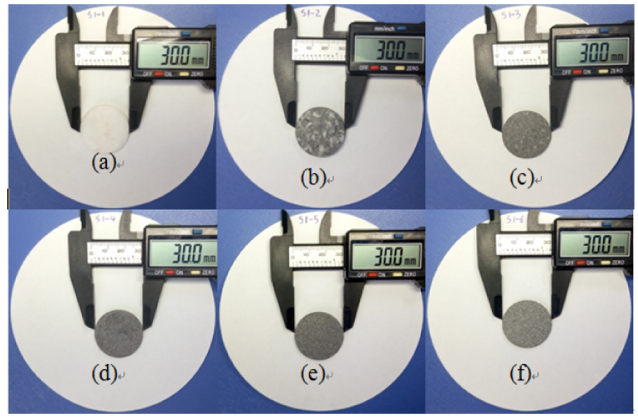

Figure 7. Sample tablets of CA/FA composites used for leakage test.

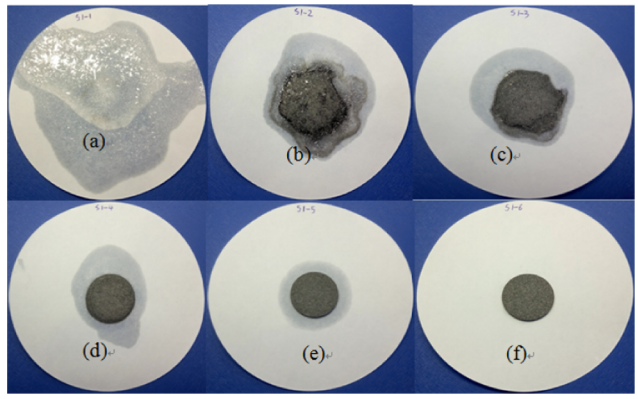

Figure 8. Leakage test results of CA/FA obtained at 60 °C.

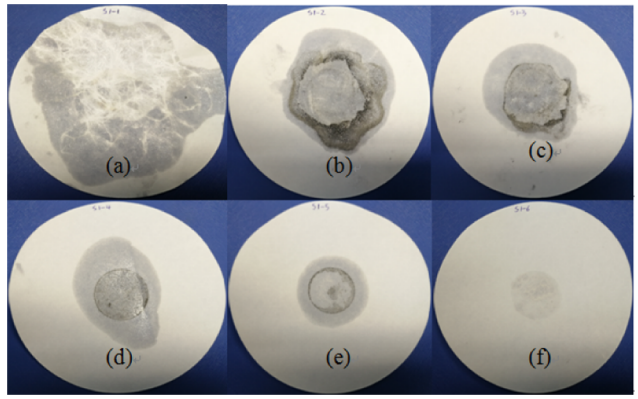

Figure 9. Liquid stains of CA in CA/FA on the filter paper after heating at 60 °C.

After cooling, the SSPCM of CA/FA/CNT was obtained. In this study, all of the samples are marked in Table 3.

The leakage area and leakage ratio of the samples are important parameters to accurately and objectively characterize the leakage of liquid CA. The results are given in Table 3, Figures 10, and 11. In Table 3, the leakage ratio is the mass of leaked CA divided by the total mass of CA in the corresponding composites.[31]

As can be seen in Figures 8 and 9, as time goes on, the leakage of CA with CA/FA composites becomes increasingly worse. Simultaneously, the leakage of CA becomes increasingly weaker with the mass fraction increment of FA due to the restriction and package of FA. And when the mass fraction of

DOI: 10.1021/acsomega.9b01746
ACS Omega 2019, 4, 14962−14969

Table 3. Basic Proportion of the CA/FA Composites

step	sample name	composition ratio of the CA/FA composite	leakage ratio (%)	leakage area of the sample (cm^2)
1	S1-1	Pure CA	46.07	72.34
1	S1-2	60% CA + 40% FA	31.56	47.76
1	S1-3	50% CA + 50% FA	27.87	34.19
1	S1-4	40% CA + 60% FA	16.42	24.62
1	S1-5	30% CA + 70% FA	9.67	18.09
1	S1-6	20% CA + 80% FA	3.17	3.80
2	S2-1	20% CA + 80% FA + CNT	0	0

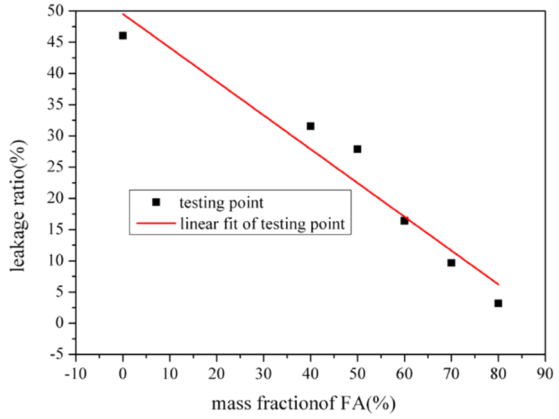

Figure 10. Leakage area of CA/FA composites with different mass fractions of FA.

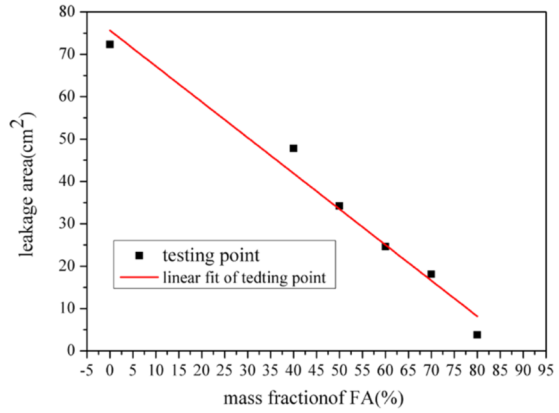

Figure 11. Leakage ratio of CA/FA composites with different mass fractions of FA.

FA is more than 60%, the composites start to keep the shapes. Yet the leakage of CA is serious even though the mass fraction of FA is up to 70%, which indicates that the package efficiency of FA is not very good. This means that raw FA is suitable for ingredients material in the whole building material application rather than an aggregate material. Meanwhile, the S1-6 sample with 20/80 wt % composite which has no liquid leakage is characterized as SSPCM in Figure 7. However, the liquid stain of the S1-6 sample shows a little liquid leakage and can be negligible. Hence, the S1-6 sample was characterized as SSPCM used in this study.

It can be seen from Figure 10 that there is a good linear relationship between the leakage area and mass fraction of FA. Namely, the leakage ratio of CA/FA samples decreases with increasing mass fraction of FA. And a similar relationship can be found between the leakage ratio and mass fraction of FA in the CA/FA composites in Figure 11. The above-mentioned relationships can be described by the following formulations: $Y_1 = -0.5416X_1 + 49.5363$, $R^2 = 0.9312$, where Y_1 stands for the leakage ratio of sample (cm^2) and X_1 stands for the mass fraction of the sample (%); $Y_2 = -0.8433X_2 + 75.6295$, $R^2 = 0.9712$, where Y_2 stands for the leakage area of the sample (cm^{-2}) and X_2 stands for the mass fraction of the sample (%). Clearly, the leakage area and the leakage ratio of the CA/FA sample with 80% mass fraction FA are very small and negligible. Moreover, these may provide relatively accurate and objective parameters to evaluate the leakage of PCM composites.

4.3. Characterization of SSPCM. The surface morphologies of CA, CA/FA, and CA/FA/CNT were researched using a scanning electron microscope. The chemical compatibility between the components of composites was studied by FTIR in the wavenumber range of 400−4000 cm^{-1}, with a resolution of 2 cm^{-1} using KBr pellets. The thermal stabilities of CA, CA/FA, and CA/FA/CNT SSPCM were measured by thermogravimetric analysis (TGA, from 20 to 600 °C). The temperature fluctuation was 0.1 °C, and the accuracy of DSC was 0.1%. The phase change temperature and latent heat of CA, CA/FA, and CA/FA/CNT SSPCM were determined by differential scanning calorimetry (DSC), and the measurement experiments were performed at the heating/cooling rate of 10 °C min^{-1} under N_2 gas atmosphere in the temperature range of 10−60 °C. In addition, to examine the effect of enhanced thermal conductivity on the heat-adsorbing and -releasing time of CA, CA/FA, and CA/FA/CNT SSPCM, continuous cooling curve tests were carried out by the intelligent paperless recorder in the range of −10 to 60 °C. The thermal storage and release performances were determined by taking advantage of the intelligent paperless recorder.

AUTHOR INFORMATION

Corresponding Authors

*E-mail: xb.gu@siat.ac.cn (X.G.).
*E-mail: zhang_zk@163.com (Z.Z.).

ORCID

Peng Liu: 0000-0002-8728-1209
Liang Bian: 0000-0002-2769-7018

Notes

The authors declare no competing financial interest.

ACKNOWLEDGMENTS

This work was supported by the National Natural Science Foundation of China (41831285), the Opening Project of Key Laboratory of Solid Waste Treatment and Resource Recycle, Ministry of Education (18zxk03), Hebei Key Technology R&D Program of the Agency of Hebei province (17214016), Science and technology research Youth Fund Project of Hebei Province Higher Education (QN2018124), the special funding of Guiyang Science and Technology Bureau and Guiyang University (GYU-KYZ(2019~2020)DT-13), Science and Technology Cooperation Program of Guizhou province (Qian Kehe LH[2015]7302), Hebei Provincial Natural Science Foundation Youth Fund(E2019403135), and Ph.D. Research Startup Foundation of Hebei GEO University (BQ2017020, BQ2017021).

DOI: 10.1021/acsomega.9b01746
ACS Omega 2019, 4, 14962−14969

REFERENCES

(1) Sarı, A.; Bicer, A.; Al-Sulaiman, F.; Karaipekli, A.; Tyagi, V. Diatomite/CNTs/PEG composite PCMs with shape-stabilized and improved thermal conductivity: preparation and thermal energy storage properties. *Energy Build.* **2018**, *164*, 166−175.

(2) Amin, M.; Putra, N.; Kosasih, E.; Prawiro, E.; Luanto, R.; Mahlia, T. Thermal properties of beeswax/graphene phase change material as energy storage for building applications. *Appl. Therm. Eng.* **2017**, *112*, 273−280.

(3) Karaipekli, A.; Bicer, A.; Sarı, A.; Tyagi, V. Thermal characteristics of expanded perlite/paraffin composite phase change material with enhanced thermal conductivity using carbon nanotubes. *Energy Convers. Manage.* **2017**, *134*, 373−381.

(4) Zhang, H.; Gao, X.; Chen, C.; Xu, T.; Fang, Y.; Zhang, Z. A capric−palmitic−stearic acid ternary eutectic mixture/expanded graphite composite phase change material for thermal energy storage. *Composites, Part A* **2016**, *87*, 138−145.

(5) Sarı, A.; Biçer, Al.; Hekimoğlu, G. Effects of carbon nanotubes additive on thermal conductivity and thermal energy storage properties of a novel composite phase change material. *J. Compos. Mater.* **2018**, *53*, 1−14.

(6) Konuklu, Y.; Unal, M.; Paksoy, H. Microencapsulation of caprylic acid with different wall materials as phase change material for thermal energy storage. *Sol. Energy Mater. Sol. Cells* **2014**, *120*, 536−542.

(7) Siddiqui, M.; Sun, D. Computational analysis of effective thermal conductivity of microencapsulated phase change material coated composite fabrics. *J. Compos. Mater.* **2014**, *49*, 2337−2348.

(8) Sarı, A. Fabrication and thermal characterization of kaolin-based composite phase change materials for latent heat storage in buildings. *Energy Build.* **2015**, *96*, 193−200.

(9) Liu, S.; Yang, H. Composite of coal-series kaolinite and capric-lauric acid as form-stable phase-change material. *Energy Technol.* **2015**, *3*, 77−83.

(10) Lv, P.; Liu, C.; Rao, Z. Review on clay mineral-based form-stable phase change materials: preparation, characterization and applications. *Renewable Sustainable Energy Rev.* **2017**, *68*, 707−726.

(11) Sobolciak, P.; Karkri, M.; Al-Maadeed, M.; Krupa, I. Thermal characterization of phase change materials based on linear low-density polyethylene, paraffin wax and expanded graphite. *Renewable Energy* **2016**, *88*, 372−382.

(12) Liu, S.; Han, L.; Xie, S.; Jia, Y.; Sun, J.; Jing, Y.; Zhang, Q. A novel medium-temperature form-stable phase change material based on dicarboxylic acid eutectic mixture/expanded graphite composites. *Sol. Energy* **2017**, *143*, 22−30.

(13) Ramakrishnan, S.; Wang, X.; Sanjayan, J. Thermal enhancement of paraffin/hydrophobic expanded perlite granular phase change composite using graphene nanoplatelets. *Energy Build.* **2018**, *169*, 206−215.

(14) Karaipekli, A.; Sarı, A. Preparation, thermal properties and thermal reliability of eutectic mixtures of fatty acids/expanded vermiculite as novel form-stable composites for energy storage. *J. Ind. Eng. Chem.* **2010**, *16*, 767−773.

(15) Jeong, S.; Jeon, J.; Chung, O.; Kim, S.; Kim, S. Evaluation of PCM/diatomite composites using exfoliated graphite nanoplatelets (xgnp) to improve thermal properties. *J. Therm. Anal. Calorim.* **2013**, *114*, 689−698.

(16) Deng, Y.; Li, J.; Qian, T.; Guan, W.; Wang, X. Preparation and characterization of KNO_3/diatomite shape-stabilized composite phase change material for high temperature thermal energy storage. *J. Mater. Sci. Technol.* **2016**, *33*, 198−203.

(17) Liu, Z.; Hu, D.; Lv, H.; Zhang, Y.; Wu, F.; Shen, D.; Fu, P. Mixed mill-heating fabrication and thermal energy storage of diatomite/paraffin phase change composite incorporated gypsum-based materials. *Appl. Therm. Eng.* **2017**, *118*, 703−713.

(18) Liu, P.; Gu, X.; Bian, L.; Cheng, X.; Peng, L.; He, H. Thermal properties and enhanced thermal conductivity of capric acid/diatomite/carbon nanotube composites as form-stable phase change materials for thermal energy storage. *ACS Omega* **2019**, *4*, 2964−2972.

(19) Sarı, A.; Bicer, A.; Al-Ahmed, A.; FahadAl-S, A.; HasanZahir, M.; Mohamed, S. Silica fume/capric acid-palmitic acid composite phase change material doped with CNTs for thermal energy storage. *Sol. Energy Mater. Sol. Cells* **2018**, *179*, 353−361.

(20) Tang, F.; Su, D.; Tang, Y.; Fang, G. Synthesis and thermal properties of fatty acid eutectics and diatomite composites as shape-stabilized phase change materials with enhanced thermal conductivity. *Sol. Energy Mater. Sol. Cells* **2015**, *141*, 218−224.

(21) Tang, Y.; Alva, G.; Huang, X.; Su, D.; Liu, L.; Fang, G. Thermal properties and morphologies of MA-SA eutectics/CNTs as composite pcms in thermal energy storage. *Energy Build.* **2016**, *127*, 603−610.

(22) Zhang, X.; Wen, R.; Huang, Z.; Tang, C.; Huang, Y.; Liu, Y.; Fang, M.; Wu, X.; Min, X.; Xu, Y. Enhancement of thermal conductivity by the introduction of carbon nanotubes as filler in paraffin/expanded perlite form-stable phase-change materials. *Energy Build.* **2017**, *149*, 463−470.

(23) Li, M.; Guo, Q.; Nutt, S. Carbon nanotube/paraffin/montmorillonite composite phase change material for thermal energy storage. *Sol. Energy* **2017**, *146*, 1−7.

(24) Chen, Y.; Zhang, Q.; Wen, X.; Yin, H.; Liu, J. A novel CNT encapsulated phase change material with enhanced thermal conductivity and photo-thermal conversion performance. *Sol. Energy Mater. Sol. Cells* **2018**, *184*, 82−90.

(25) Zhang, Q.; Liu, J. Sebacic acid/CNT sponge phase change material with excellent thermal conductivity and photo-thermal performance. *Sol. Energy Mater. Sol. Cells* **2018**, *179*, 217−222.

(26) Xu, D.; Yang, H.; Ouyang, J.; Fu, L.; Chen, D.; et al. Lauric acid hybridizing fly ash composite for thermal energy storage. *Minerals* **2018**, *8*, 161−169.

(27) Pilehvar, S.; Cao, V.; Szczotok, A.; Carmona, M.; Valentini, L.; Lanzón, M.; Pamies, R.; Kjøniksen, A. Physical and mechanical properties of fly ash and slag geopolymer concrete containing different types of micro-encapsulated phase change materials. *Constr. Build. Mater.* **2018**, *173*, 28−39.

(28) Liu, L.; Peng, B.; Yue, C.; Guo, M.; Zhang, M. Low-cost, shape-stabilized fly ash composite phase change material synthesized by using a facile process for building energy efficiency. *Mater. Chem. Phys.* **2019**, *222*, 87−95.

(29) Genc, Z.; Canbay, C.; Acar, S.; Sekerci, M.; Genc, M. Preparation and thermal properties of heterogeneous composite phase change materials based on camphene-palmitic acid. *J. Therm. Anal. Calorim.* **2015**, *120*, 1679−1688.

(30) Song, H.; Yum, W.; Oh, J.; Park, I.; Yoon, S. *Development of Fly Ash-Based Aggregate Using Phase Change Materials and Thermal Performance Analysis Using TGA*; Korea Concrete Institute, 2018; Vol. *30*, pp 147−148.

(31) Ramakrishnan, S.; Wang, X.; Sanjayan, J.; Wilson, J. Assessing the feasibility of integrating form-stable phase change material composites with cementitious composites and prevention of PCM leakage. *Mater. Lett.* **2017**, *192*, 88−91.

(32) Wen, R.; Zhang, X.; Huang, Z.; Fang, M.; Liu, Y.; Wu, X.; Min, X.; Gao, W.; Huang, S. Preparation and thermal properties of fatty acid/diatomite form-stable composite phase change material for thermal energy storage. *Sol. Energy Mater. Sol. Cells* **2018**, *178*, 273−279.

(33) Li, X.; Chen, H.; Liu, L.; Lu, Z.; Sanjayan, J.; Duan, W. Development of granular expanded perlite/paraffin phase change material composites and prevention of leakage. *Sol. Energy* **2016**, *137*, 179−188.

(34) Sarı, A.; Karaipekli, A. thermal properties and thermal reliability of capric acid/expanded perlite composite for thermal energy storage. *Mater. Chem. Phys.* **2008**, *109*, 459−464.

(35) Mei, D.; Zhang, B.; Liu, R.; Zhang, Y.; Liu, J. Preparation of capric acid/halloysite nanotube composite as form-stable phase change material for thermal energy storage. *Sol. Energy Mater. Sol. Cells* **2011**, *95*, 2772−2777.

DOI: 10.1021/acsomega.9b01746
ACS Omega 2019, 4, 14962−14969

(36) Karaipekli, A.; Sarı, A. Capric-myristic acid/vermiculite composite as form-stable phase change material for thermal energy storage. *Sol. Energy* **2009**, *83*, 323−332.
(37) Hawes, D.; Feldman, D.; Banu, D. Latent heat storage in building materials. *Energy Build.* **1993**, *20*, 77−86.
(38) Memon, S.; Liao, W.; Yang, S.; Cui, H.; Shah, S. Development of composite PCMs by incorporation of paraffin into various building materials. *Materials* **2015**, *8*, 499−518.
(39) Biçer, A.; Sarı, A. New kinds of energy-storing building composite PCMs for thermal energy storage. *Energy Convers. Manage.* **2013**, *69*, 148−156.
(40) Fang, G.; Li, H.; Cao, L.; Shan, F. Preparation and thermal properties of form-stable palmitic acid/active aluminum oxide composites as phase change materials for latent heat storage. *Mater. Chem. Phys.* **2012**, *137*, 558−564.
(41) Lv, P.; Liu, C.; Rao, Z. Experiment study on the thermal properties of paraffin/kaolin thermalenergy storage form-stable phase change material. *Appl. Energy* **2016**, *182*, 475−487.

DOI: 10.1021/acsomega.9b01746
ACS Omega 2019, 4, 14962−14969